

8-30-2024

Thermomechanical Analysis of Biomass Plastic Composite (BPC)

Solomon Chijioke Madu

Department of Metallurgical and Materials Engineering, Faculty of Engineering, African Centre for Sustainable Power and Energy Development (ACE-SPED), University of Nigeria, 410001 Nsukka, Nigeria, solomon.madu@unn.edu.ng

Victor Sunday Aigbodion

Department of Metallurgical and Materials Engineering, Faculty of Engineering, African Centre for Sustainable Power and Energy Development (ACE-SPED), University of Nigeria, 410001 Nsukka, Nigeria and Faculty of Engineering and Built Environment, University of Johannesburg, P. O. Box 534 Auckland Park, South Africa., victor.aigbodion@uun.edu.ng

Ikechukwu Ike-eze

Department of Metallurgical and Materials Engineering, Faculty of Engineering, African Centre for Sustainable Power and Energy Development (ACE-SPED), University of Nigeria, 410001 Nsukka, Nigeria, ikechukwu.ezema@uun.edu.ng

Follow this and additional works at: <https://scholarhub.ui.ac.id/mjt>

 Part of the [Polymer and Organic Materials Commons](#)

Recommended Citation

Madu, Solomon Chijioke; Aigbodion, Victor Sunday; and Ike-eze, Ikechukwu (2024) "Thermomechanical Analysis of Biomass Plastic Composite (BPC)," *Makara Journal of Technology*. Vol. 28: Iss. 2, Article 5. DOI: 10.7454/mst.v28i2.1680
Available at: <https://scholarhub.ui.ac.id/mjt/vol28/iss2/5>

This Article is brought to you for free and open access by the Universitas Indonesia at UI Scholars Hub. It has been accepted for inclusion in Makara Journal of Technology by an authorized editor of UI Scholars Hub.

Thermomechanical Analysis of Biomass Plastic Composite (BPC)

Cover Page Footnote

The first author wishes to thank the African-German Network of Excellence in Science (AGNES) for granting him a Mobility Grant in 2021; the Grant was generously sponsored by German Federal Ministry of Education and Research and supported by the Alexander von Humboldt Foundation. The authors also wish to appreciate the support and the facilitating environment provided by the Africa Centre of Excellence for Sustainable Power and Energy Development (ACE-SPED), University of Nigeria. TETFund supported research project no. (TETF/DR&D/CE/UNI/NSUKKA/BR/2024/VOL.IB).

Thermomechanical Analysis of Biomass Plastic Composite (BPC)

Solomon C. Madu^{1*}, Victor S. Aigbodion^{1,2}, and Ikechukwu Ike-eze¹

1. Department of Metallurgical and Materials Engineering, Faculty of Engineering,
African Centre for Sustainable Power and Energy Development, University of Nigeria,
Nsukka 410001, Nigeria

2. Faculty of Engineering and Built Environment, University of Johannesburg,
P.O. Box 534 Auckland Park, South Africa

*E-mail: solomon.madu@unn.edu.ng

Abstract

High-performance electrical insulation material can be manufactured using biomass plastic composite (BPC), which is a new type of composite material that is either made up of one or a combination of natural plant fibers/particulates, such as bamboo, cellulose fiber, rice husks, or hemp, and thermoplastic granules. In this study, the BPC composite material that was developed comprised polyethylene (PE), rice husk, and oyster shell. The results of the study showed a significant optimal improvement in the morphological, thermodynamic, and mechanical properties during the addition of 20% to 30% biomass particulates (i.e., rice husk and oyster shell). The thermogravimetric analysis, storage modulus, loss modulus, and damping factor (also known as the tangent of delta [$\tan\delta$]) values showed that compositions of the BPC material exhibited an increasing optimal thermomechanical stability when the composition of the BPC material was made with an increasing mixture of oyster shell, rice husk, and PE compared with that when only rice husk was added to PE. Similarly, the mechanical property of BPC was enhanced with 30% biomass material (i.e., rice husk and oyster shell) and 70% low-density PE plastics. This result indicated that BPC materials can be highly durable and long-lasting, as they are less prone to cracking or breaking.

Keywords: biomass, composite, loss modulus plastics, storage modulus, tangent of delta

1. Introduction

The increasing global population has led to an increased demand for both natural and synthetic products. However, the production processes of these products have resulted in a significant amount of waste material, causing environmental pollution. In addition, the progressive growth of the human population and the improper management of industrial and consumer plastics packages are leading issues of ecological and environmental imbalance [1].

Nevertheless, the impacts of plastic pollution on both the environment and people are highly visible, which poses a serious problematic challenge. The iniquitousness and massive production rate of plastic are also known to have adverse effects on the environment on account of its slow decomposition rate, which can last up to 500 years because of the strong bond between molecules [2].

Similarly, polymer material is known for its inherent poor thermal stability because of its low-temperature melting point. Therefore, this research addresses this

gap by introducing biomass particulate fillers to boost its thermal stability.

Lignocellulose is one of the biomass fillers that is the most abundant and widely utilized renewable material on earth. However, in certain countries, such as Turkey, where forest resources are scarce, the use of annual plants has become a more viable option and has significantly contributed to the economic growth and prosperity of the country [3].

Polymer composite can be fabricated by the incorporation of biomass flakes/fibers/particulates into various volumes or weight percentages. Therefore, biomass plastic composite (BPC) is a material that comprises natural fibers and animal shells or limestone as a reinforcing material, mostly using a thermoplastic resin (e.g., polypropylene [PP], polycarbonate, polyethylene terephthalate [PET], and polyethylene [PE]) as a bonding matrix. The composite material has the properties of biomass and plastic matrix, can be recycled and processed, has certain biodegradability, and is a novel environment-friendly material. At present, biomass-

reinforcing materials, such as rice husks, bagasse, hemp fibers, wood fibers, oyster shells, eggshells, snail shells, and bamboo fibers, have not been used with plastic to produce BPC. Biomass materials are low-cost (e.g., low price ratio of jute, cheap sisal hemp, wasted and abandoned biomass, and common natural fibers with the lowest price) and light natural fibers and have rich resources. The global yield of plastic wastes and biomass materials was approximately 500 billion tons/year [4]. Countries, such as Nigeria, also have rich biomass resources, which are mainly distributed across the six geopolitical zones, and the annual yield is estimated to be 2.29 billion [5]. Existing natural fibers are mainly used for producing ropes, cushions, carpets, braided fabrics, mats, brooms, brushes, mattresses, indoor decoration, and filter cloth; moreover, only a small part of the yield of fibers and shells in the world is considered, and the rest of the biomass is taken as fuels or is naturally abandoned and blindly wasted, causing environmental pollution [6, 7].

In the past, researchers used eggshells and natural fiber to reinforce thermoset polymer to form a composite material that has a successful application case [8]. However, research to use BPC materials comprising oyster shells and natural fibers, which are reinforced with PE, to produce thermoplastic composite material that would form high-strength to less-weight ratio materials has not seen a successful application case, especially when the utilization of BPC material in engineering applications considering the biomass materials (shell and fiber particulate) as the reinforcing body and either PE (high-density polyethylene [HDPE] or low-density polyethylene [LDPE]), PET, or PP as the bonding matrix has not been reported. Alternatively, the shell- and fiber-reinforced thermoset resin, which comprises unsaturated polyester, phenolic, and epoxy resins, has great potential in the current field of research investigations [9]. The alkali-treated shell and natural-fiber-reinforced unsaturated resin have mechanical properties exceeding that of wood plywood and wood chips and are close to the performance of pine wood. This finding indicates that the shell- and natural-fiber-reinforced composite material can partially replace wood or plywood as structural materials for practical application. However, the thermoset polymer composite material cannot be recycled and is unfavorable for circular economy and environmental protection.

Thermoplastics are a type of plastic polymer that softens when heated and solidifies when cooled. These materials can be repeatedly heated and cooled, i.e., melting to a liquid state when heated and returning to a solid state when cooled [10].

Thermoplastic materials have the unique property of being able to undergo multiple cycles of heating and cooling without any permanent change. Essentially, thermoplastic materials can melt when heated and solidify again when cooled. Some common examples of thermoplastics include PET, HDPE, polyvinyl chloride, LDPE, PP, and polystyrene [11].

In the analysis of the thermal properties of the polymer composite, hydrophilicity and poor thermal stability of biomass materials fillers are ineligible during the preparation of the polymer composite. Dynamic mechanical analysis (DMA) is considered to be the most important technique in thermal investigation [12]. The modulus property and viscoelastic behavior of a wide range of materials as a function of frequency or temperature can be investigated when materials are deformed because of the influence of a periodic force or displacement [13]. This parameter ensures that appropriate materials with the correct mechanical properties are used. Young's modulus (E) or shear modulus can be evaluated using a dynamic testing machine under different measurement conditions. The graph illustrates the outcomes of DMA measurements of BPC under shear conditions.

Modern electrical materials, such as plastic material, undergo various stresses at different frequencies. The viscoelastic behavior of these materials and their modulus values can be characterized using DMA measurements. The storage modulus (E'), loss modulus (E''), and mechanical damping parameter (tangent of delta [$\tan\delta$]) are depicted in the graphs as they vary with temperature. These values are obtained through a simple method where a sample is subjected to small cyclic deformations. The capability to analyze the behavior of the material when subjected to various factors, such as stress, temperature, frequency, and other parameters, is facilitated by this process. In addition, the term is commonly used to describe the instrument that conducts these tests. Hence, DMA is a technique used to assess the viscoelastic characteristics of materials, specifically polymers and composites, by measuring the stress or strain that arises from subjecting the sample to dynamically changing stress or strain.

2. Experimental

Materials and method. PE was collected from environmental waste and used as thermoplastic resin. Biomass materials, such as rice husk and oyster shells, were used as natural fillers, which were collected from the rice-harvested farmland and on the shore of river-line areas, respectively.



Figure 1. Illustration of Biomass Plastic Composite (BPC) Fabrication

The biomass materials were dried at 80 °C, ground using a SEVA hammer mill, and passed through an 80 mesh sieve. PE was granulated and mixed with the pulverized biomass materials at different percentage proportions in a ribbon mixer. The mixed BPC underwent screw extrusion at different barrel heating zones, which were maintained at 180 °C for 180 s. Afterward, the mixed BPC was placed in a mold and manually pressed. The mold was fabricated using a 20mm × 20 mm × 12 mm aluminum metal sheet, and a silicon spray cover was used to facilitate the unmolding of the BPC sample from the manual press. After the formation of the BPC, the casting was slowly cooled, leading to an easy removal of the sheet. For DMA, the resulting sheets were cut into 35 mm × 12 mm × 0.3 mm specimens.

Characterization. DMA of the BPC samples was conducted using the TA Instruments DMA 2980 apparatus at a frequency of 1 Hz in a single cantilever bending mode. The BPC samples underwent testing at temperatures of 35 °C to 120 °C.

Differential scanning calorimetry was conducted using the TA Instruments DSC 2910. Small fragments (milligrams) of each composite were subjected to gradual heating at a rate of 12 °C/min, ranging from 26 °C to 410 °C under atmospheric air conditions. The decline in the properties of BPC under thermal conditions was evaluated by conducting thermogravimetric analysis (TGA). The analysis was performed using the TA Instruments 2950 under atmospheric air conditions at a heating rate of 10 °C/min. To investigate the scattering of biomass particulates within the PE matrix, we captured a series of optical microscopic images using the Nikon Optiphot 2 Pol in transmitted light mode.

Scanning electron microscopy (SEM) of the BPC samples was conducted by cutting the composite sample into small pieces (e.g., 1 cm × 1 cm). The surface of the BPC sample was polished using progressively finer grits, and the sample was coated with a conductive material (e.g., gold and carbon) to prevent charging.

The mechanical property of BPC material was also characterized using a universal tensile testing machine



Figure 2. Illustration of the Dynamic Mechanical Analysis (DMA) Testing Approach Conducted on the BPC

(UTTM). The UTTM evaluated the mechanical properties of BPC by cutting the composite sample into dog-bone-shaped specimens, which is a standard test method for tensile properties of plastics (ASTM D638), typically 150 mm × 19 mm × 3 mm (length × width × thickness), and selecting and applying the appropriate load cell capacity after the sample had been secured in grips to ascertain material development and optimization for various applications.

3. Results and Discussion

Morphological characteristics. This section presents the microstructure and fracture morphology of BPCs at low temperatures as the content of the biomass particulate increases. The SEM images (Figure 3) revealed that biomass particulates have a generally semitransparent film-like appearance with twists and turns. In most cases, biomass particulates are stacked in multiple layers, overlapping each other. The SEM images showed that, as the biomass particulate content increased, a stable chain of heat insulation network was formed within the BPCs. However, when the packing material was further increased, the biomass particulates formed a larger structure, which resulted in agglomeration within the PE matrix (refer to Figure 4). The dispersion of biomass particulates in the confines of the PE matrix is important in enhancing the heat insulation of the BPCs. The diffusion of phonons enables effective thermal insulation in biomass particulates. Nevertheless, excessive overlapping and agglomeration of biomass particulates can lead to defects in BPCs, potentially disrupting the formation of network cross-linking and causing a decline in mechanical properties [13]. This section presents the microstructure and fracture morphology of BPCs at low temperatures as the content of the biomass particulate increases.

Thermal Properties

Effect of biomass particulate contents on the thermal insulation of polymer. The thermal insulation of BPCs was significantly improved when (biomass) oyster shell and rice husk particulates were added to the samples (check Figure 9). As the biomass content increased to

12wt%, the thermal conductivity of BPCs increased by a staggering 258.9%. In comparison to graphite [14], the addition of biomass particulates had a more pronounced effect on enhancing the heat insulation capability of BPCs. The enhanced heat insulation in biomass can be primarily attributed to phonon diffusion, which is also the main mechanism for modifying BPC heat insulation [15]. Observations of the SEM micrographs reveal multiple interfaces between the biomass fillers, RH, OS, and PE matrix, resulting in increased contact resistance and phonon scattering at these interfaces. However, as the mass ratio of biomass increases, the interfacial thermal contact resistance decreases, thereby reducing the scattering of interfacial phonons and ultimately improving the thermal insulation of BPC.

Therefore, improved dispersion may result in the enhancement of the thermic contact impedance that separates the fillers and the matrix of the polymer. These factors are crucial in achieving a higher level of thermal insulation enhancement in nanocomposites.

TGA of the surface-functionalized BPC was conducted to determine their thermal behavior and level of functionalization, as shown in Figure 9. TGA revealed that biomass particulates exhibit a distinct response to thermal decomposition and thermal stability compared with PE [14]. Biomass particulates exhibit high thermal stability up to 400 °C with 1.3% weight loss. Previous studies have shown that PE experiences negligible weight loss up to 600 °C [15].

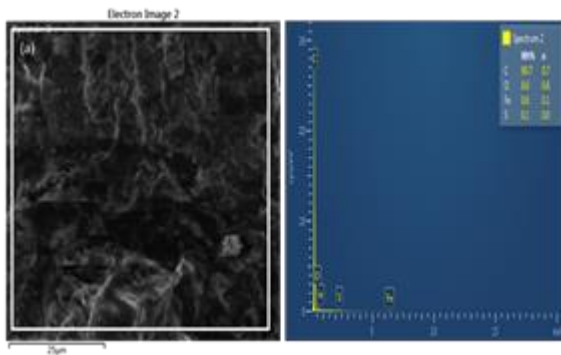


Figure 3. SEM/EDS Micrographs of BPCs with the Addition of Biomass Particulates

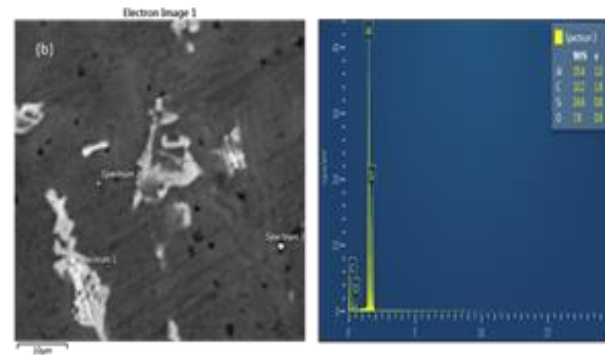


Figure 4. SEM/EDS Micrographs of BPCs with the Addition of 30% Biomass Particulates

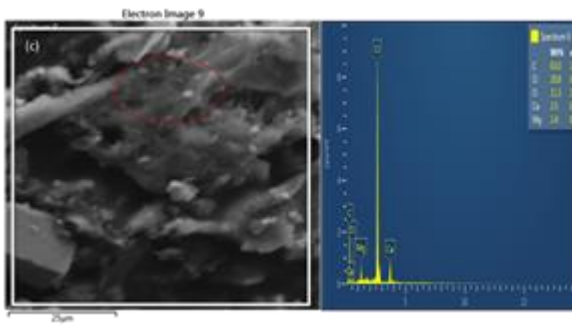


Figure 5. SEM/EDS Micrographs of BPCs with the Addition of 40% Biomass Particulates

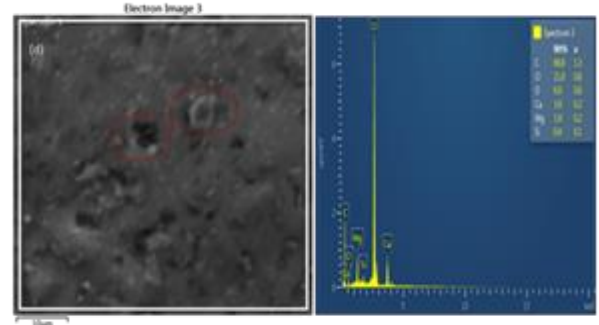


Figure 6. SEM/EDS Micrographs with the Addition of 30% Biomass Particulates (Rice Husks and Oyster Shell) in Polymer

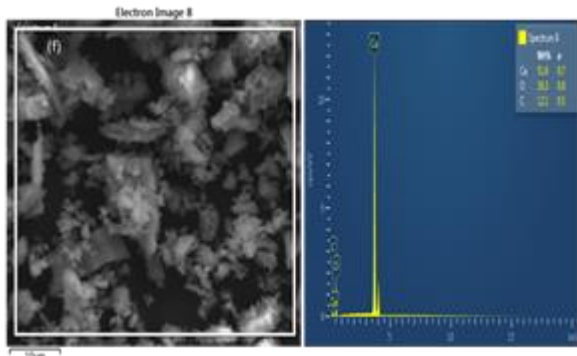


Figure 7. SEM/EDS Image of Oyster Shells

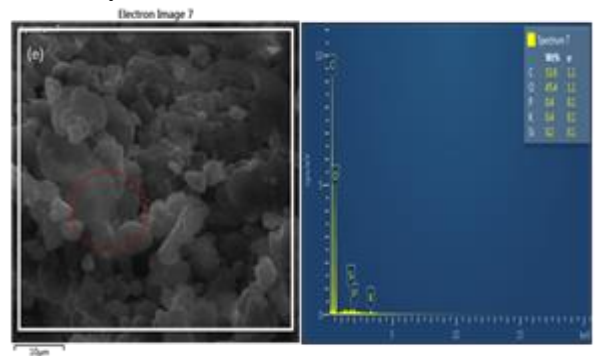


Figure 8. SEM/EDS Image of Rice Husks

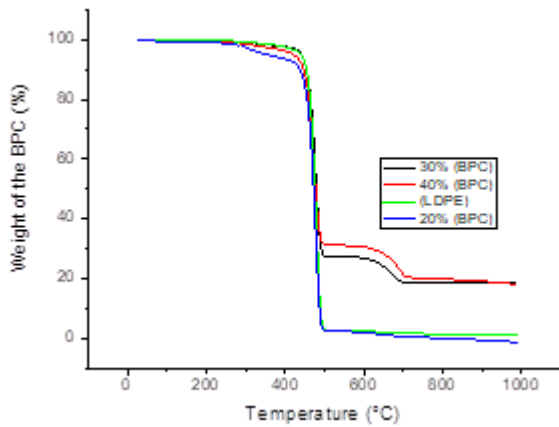


Figure 9. Thermogravimetric Analysis Curves of LDPE and BPC Biomass at 40% of Particulate Fillers

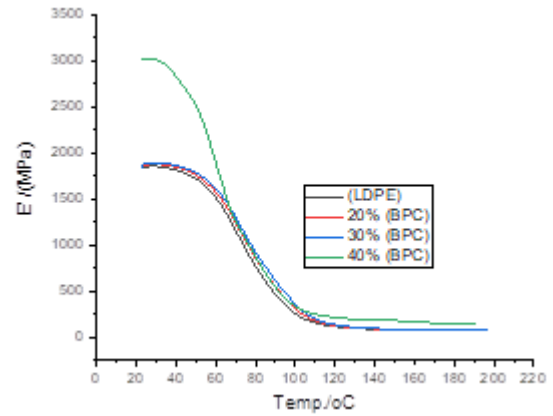


Figure 10. Storage Modulus Curves Obtained by DMA Conducted on BPC

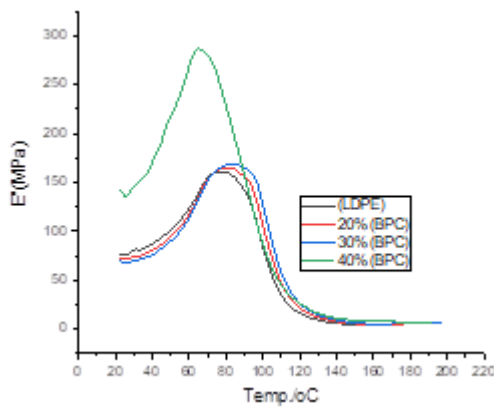


Figure 11. Loss Modulus Curves Obtained by DMA of BPC

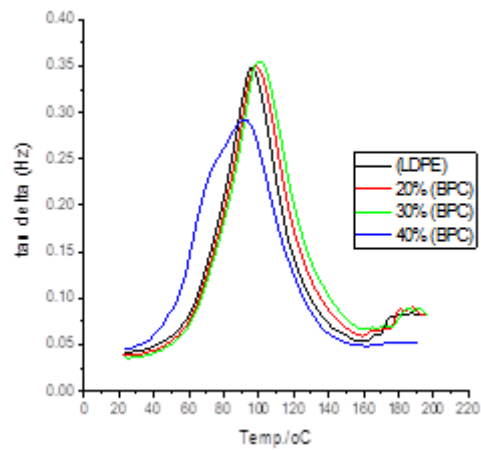


Figure 12. Tan delta Curves Obtained by DMA of BPC

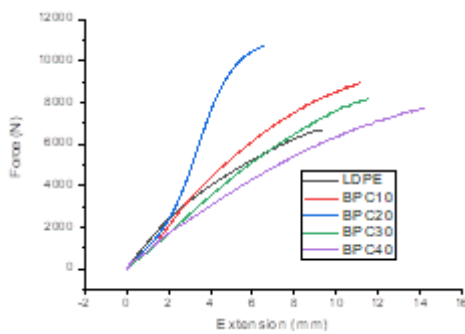


Figure 13. Load Extension Graph

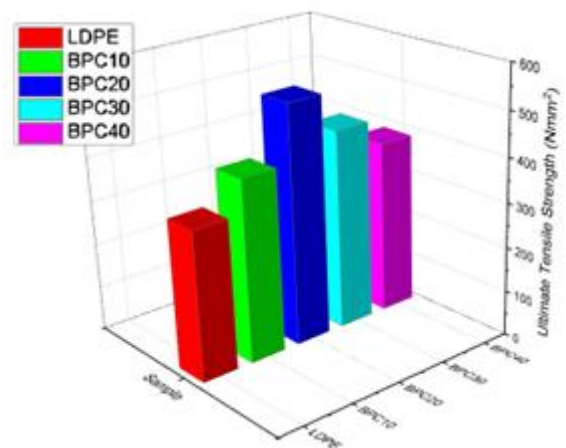


Figure 14. Ultimate Tensile Strength (N/mm²)

Therefore, the thermal stability of the BPC materials increased as the biomass particulate percentage increased, as indicated by the TGA curve shown in Figure 9. The temperature of decomposition is another instance in which the trend showcases itself when the materials are

recorded to have given up 30% in weight. For instance, pure PE (Sample A) experiences a 30% weight loss at 269 °C. A similar weight loss occurs at 368 °C with 30% biomass fiber (Sample C). This increase in temperature

can be attributed to the compatibility between the rice husk/oyster shell fiber and the plastic matrix [16, 17].

The thermal disintegration of BPC involves a two-step process. In the first phase, at temperatures ranging from 125 °C to 200 °C, the bonds between adjacent polymer chains and unsaturated end groups formed during the initial and final reactions disintegrate. At this temperature range, minimal weight loss, i.e., approximately 6% to 8% of the total sample weight, occurs, indicating that only a small number of chains possess these fragile bonds [18].

The second phase commences at a temperature of 225 °C and concludes at temperatures of 310 °C for Sample P and 360 °C for Sample PRO. The procedure here is governed by the disintegration of C–C and C–H bonds, specifically involving the depolymerization of BPC initiated by the labile thermal groups. During the final polymerization process, unsaturated end groups are created through either disproportionation or the formation of head–head linkages resulting from the radical recombination in the growth stage. When subjected to high temperatures, the weakest bonds disintegrate, causing the release of volatile monomer units. This process is the inverse of polymerization [12].

Figure 10 shows the storage modulus (E') of BPC, as evaluated using DMA. The first modulus (E' at 35 °C) increases when 30% and 40% of biomass particulates are incorporated, as the fiber support enables the movement of strength at the interface. However, when greater than 45% of biomass fiber particulate is incorporated, the E' value gradually decreases at room temperature. The influence that elevated temperatures have on the behavior of the composite needs to be considered. At 70 °C, the E' value for PE without support was 1,250 MPa, whereas those for the other substances with biomass fiber particulates were significantly higher. For example, Composite PO has an E' value of 1,500 MPa, which is 140% higher, and Composite PRO has an E' value of 1,750 MPa, which is 213% higher.

As E' decreases in each of the composites, the loss modulus (E'') increases to its maximum value, as shown in Figure 11, which occurs at elevated temperatures with the increased movement of polymeric chains. Several authors proposed the use of the maximum E'' value as the transition temperature (T_g), whereas other authors associated this transition with the $\tan\delta$ peak. The reinforced BPC in either event exhibits higher transition temperatures, as shown in Figure 11.

The ratio of the loss energy and storage energy (E''/E'), also known as $\tan\delta$, yields the damping factor. E''/E' also relies on the level of adhesion between the biomass particulate and the matrix.

Therefore, the lack of a strong bond between the fiber and the matrix will result in higher $\tan\delta$ values [19]. Figure 12 illustrates that the reinforced composites exhibit lower energy dissipation coefficients, indicating a favorable interface between the biomass particulate and the matrix. Damping in these materials was observed to have significantly reduced because of the presence of polymeric chains attached to the biomass particulates, which restrict their mobility and decrease friction among them. Alternatively, specimens with a 40% weight fraction exhibited a lower elastic modulus than specimens with 10%, 20%, 30%, and 0% weight fractions, despite having better mechanical characteristics than the unreinforced specimens. This observation is consistent with the findings of other researchers [20] who proposed that this phenomenon can be attributed to the agglomeration and exfoliation of biomass particulates, resulting in reduced mobility of polymer chains under tensile loads. Typically, agglomeration negatively impacts the mechanical characteristics of a polymer composite material because it creates local stress concentrations and promotes particle interlocking, thereby improving the rate at which the polymer chain moves and exacerbating the concentration of the stress effect caused by the inclusion of fillers in PE. Finally, the introduction of biomass particulates serves as a crack resistor by undergoing plastic deformation before failure (through debonding and dimensional changes), which may elucidate the increase in strain observed after a 20% weight fraction of biomass particulates.

Tensile strength. The findings of the tensile strength test that was conducted are depicted in Figure 13. The composite samples were tested under identical situations, and the resulting values indicate that specimens with a 20% weight fraction exhibit higher tensile strength and elastic modulus than the unreinforced specimens.

A decline in mechanical properties was observed when a high percentage of additives was used. Thicker viscosity and consistency were observed in the mixture containing 40% additive when compared with the mixture containing 30% additive. In addition, poor adhesion between the two phases of 40% biomass particulates and LDPE was observed, which resulted in an uneven distribution of the biomass particulates throughout the matrix and ultimately led to a decrease in tensile strength. This finding is consistent with those of the studies conducted by Balasubramanian *et al.* [21] who reviewed the role, effect, and influence of micro and nano-fillers on various properties of polymer composite. His studies indicated that the tensile strength was directly proportional to the amount of particulate filler used. His findings further indicated that the amount of filler present had a direct impact on the tensile strength. Notably, the elastic modulus and tensile strength started to decrease at 10% weight fraction and further decreased at 114% weight fraction. These decreases could be attributed to the reasons explained previously.

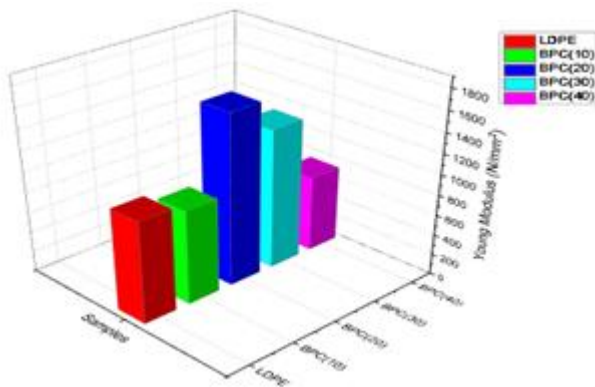


Figure 15. Illustration of the elastic modulus of BPC

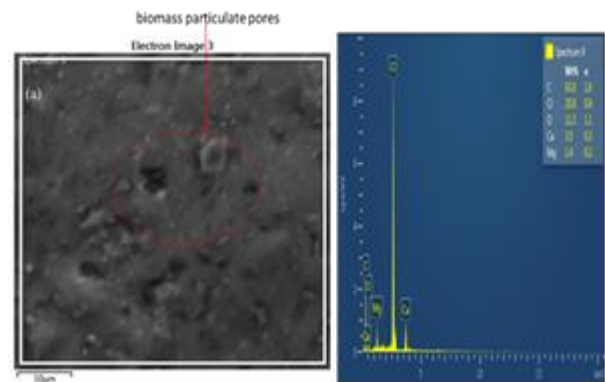


Figure 16. SEM image of 40% biomass-reinforced recycled LDPE

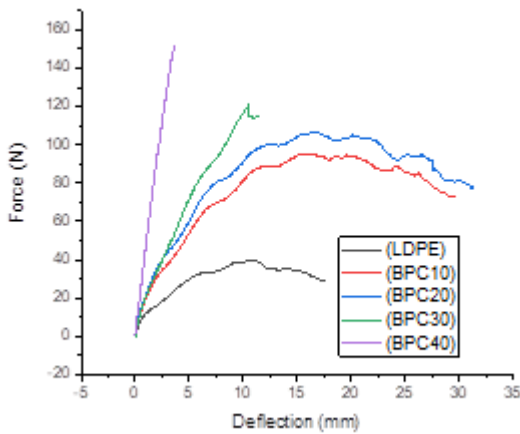


Figure 17. Flexural strength graph of BPC

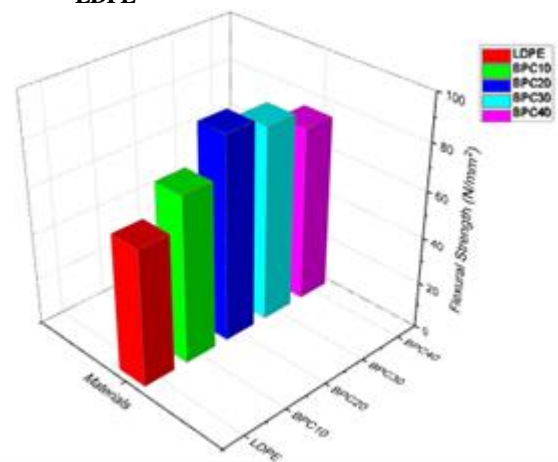


Figure 18. Illustration of the bar chart of the flexural strength of BPC

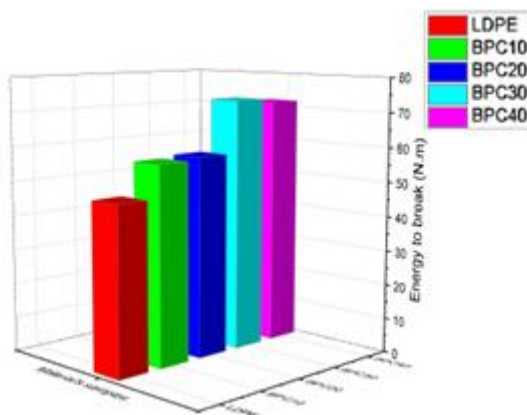


Figure 19. Illustration of the bar chart of the impact strength of BPC

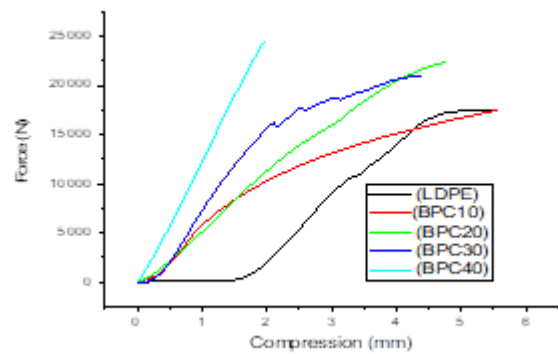


Figure 20. Graph of the compressive strength of different samples of BPC

In addition, the tensile characteristics of BPC samples derived from oyster shell and rice husk particulates were compared with those of recycled LDPE. The ultimate tensile strength of recycled LDPE was measured at 334.775 MPa. For the BPC samples, the ultimate tensile strengths of BPC10, BPC20, BPC30, and BPC40 were recorded as 408.261, 536.027, 447.379, and 387.941

MPa, respectively. Among these, BPC20 exhibited the highest tensile strength, showing a 24% increase compared with the 334.775 MPa of recycled LDPE.

The elastic modulus of recycled LDPE was 1,000.754 MPa, whereas the elastic moduli of BPC10, BPC20, BPC30, and BPC40 were 922.912, 1,668.311, 1,367.231,

and 747.348 MPa, respectively. The maximum elastic modulus was observed in BPC20, indicating a 34% enhancement of Young's modulus. This finding indicates that the mechanical characteristics of the composite rely on how evenly the filler particles are dispersed within the matrix and the level to which the particles clump together. Another aspect that affects the tensile strength of a composite is how stress is transferred through interfacial bonding. If the recycled LDPE successfully fills the biomass particulate pores and effectively transfers stress, then it significantly increases the likelihood of enhancing the mechanical properties of the composite by providing rigidity.

The high tensile strength of the composite derived from 20% particulate can be attributed to several factors. One key factor is the uniform and homogenous dispersion of particulate in the LDPE matrix, preventing the agglomeration of particles and facilitating a good stress transfer mechanism. Another contributing factor is the proper filling of the biomass particulate pores by the recycled LDPE, which promotes strong interfacial bonding. These findings are supported by the SEM image of BPC20. However, when 40% particulate was added, the tensile strength decreased because of the nonuniform dispersion of the particulates, increased particle agglomeration, and weakened interfacial bonding [22].

In terms of elastic modulus, biomass particulates exhibit minimal deformation and are highly rigid, which restrict the mobility of recycled LDPE macromolecules, resulting in increased elastic modulus when biomass particulates are added to recycled LDPE, ranging from 0% to 20% [23]. The low elastic modulus of BPC40 may have been a result of biomass particulate agglomeration and poor stress transfer between the filler particles and the matrix. The SEM images provide further insights into the factors contributing to the variation in tensile properties.

In addition, BPC20 exhibited the highest tensile modulus because it had the most interlocking of biomass particulate pores with the recycled LDPE, resulting in rigidity and stiffness. Alternatively, BPC10 had the lowest tensile modulus because of the lower biomass particulate loading, whereas BPC40 exhibited a decrease in tensile modulus because of agglomeration.

Figure 16 shows the SEM images of the tensile cross-sectional fracture surface of both the recycled LDPE and biomass particulate composites. Figure 16 also shows the smooth structure of the recycled LDPE. The porous structure of biomass was evident in the 20% biomass-reinforced composite or BPC20. The majority of the biomass particulate pores are uniformly filled with recycled LDPE, resulting in a better distribution of filler particles, which leads to a strong physical-mechanical interlocking structure [24]. The efficient transfer of stress

between the particulates and the recycled LDPE contributes to BPC20 exhibiting the highest tensile strength among all samples. The SEM image of BPC40 reveals signs of agglomeration and clusters of biomass particulates, which diminishes its tensile strength.

Flexural strength. Figure 3.15 compares the flexural properties of the recycled LDPE with the biomass-particulate-derived composite samples. The flexural strength property of the recycled LDPE was measured at 58.875 MPa. The flexural properties of BPC10, BPC20, BPC30, and BPC40 were 71.568, 87.937, 83.562, and 75.500 MPa, respectively. BPC20 showed a 19% improvement in flexural strength compared with the recycled LDPE, exhibiting the highest flexural strength among the samples. The trend of the flexural properties mirrored that of the tensile properties.

BPC with a 20% weight fraction of filler materials exhibited high flexural strength because of their combined materials and the redistribution of stress, enhancing their suitability for high-stress applications.

The improvement in flexural characteristics resulted from the porous structure of the biomass particulates and the physical interlocking between the biomass and the recycled LDPE. During screw extrusion, the slurry LDPE was able to fill the biomass particulate pores, creating a rigid structure with strong interaction. After cooling, a robust physically interlocked structure was achieved. This enhancement enabled efficient stress transfer, leading to improved flexural properties. In addition, the dispersion of biomass particulates in the matrix played a role in the variation of flexural properties. In the case of the BPC40 composite, poor particulate dispersion or agglomeration may have caused a noticeable decrease in flexural strength and modulus.

Impact strength. The impact strengths of the recycled LDPE and BPC materials are shown in Figure 19. Specifically, the impact strength values for the recycled LDPE, BPC10, BPC20, BPC30, and BPC40 were 47.894, 57.169, 57.95, 73.099, and 74.962 N·m, respectively. Notably, the trend of impact strengths differed from that of tensile and flexural strengths. The decrease in impact strength was consistent with the behavior observed in fiber-polymer composites [25]. Notably, a decrease of approximately 25.8% in impact strength from the recycled LDPE to the BPC40 sample was observed.

The result of the impact strength test is depicted in Figure 19, indicating that the impact strength varied from 47.894 N·m for the original sample to 73.099 and 71.962 N·m for the 30% and 40% samples. The change in impact strength can be attributed to the interface between the two phases in the composite material. In addition, the clumping of biomass (oyster shell and rice husk)

particulates may have played a role in this outcome because of discontinuities and the presence of voids caused by the high concentration of biomass particulates. These factors promote stress concentrations and result in plastic deformation on a large scale before eventual fracture, leading to a high impact strength. The viscosity of the material may have also contributed to the uneven dispersion of particles.

The impact strength of a BPC material relies completely on stiffness and resilience [26]. The lower the stiffness of the material is, the higher its resilience and the greater its

impact strength, and vice versa. The stiffness of the material was determined by the movement of the recycled LDPE molecules, which, in turn, depended on the physical (mechanical) interlocking structure between the biomass particulate and the LDPE molecules. When the biomass content in the recycled LDPE matrix was 12%, the likelihood of the recycled LDPE flowing into the biomass particulate pores was reduced, resulting in increased mobility of the recycled LDPE. Thus, its capability to absorb energy during fracture propagation was enhanced, leading to higher toughness.

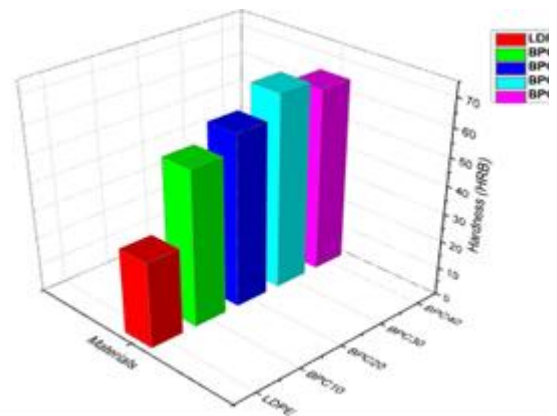
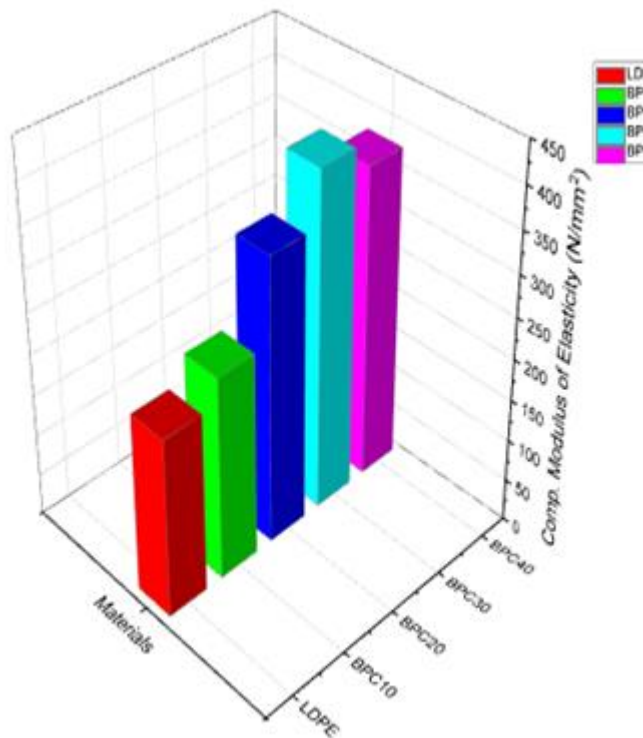


Figure 21. Illustration of the Bar Chart Showing the Compressive Elastic Modulus

Figure 22. Illustration of the Hardness of the Materials

Table 1. Summary of the Mechanical Properties of the BPC Samples

S/N	LDPE	BPC10	BPC20	BPC30	BPC40
Ultimate tensile strength (N/mm ²)	334.775	408.261	536.027	447.379	387.941
Force at peak (N)	6,695.49	8,165.213	10,720.531	8,007.588	7,758.825
Young's modulus (N/mm ²)	1,000.754	922.912	1,668.311	1,367.231	747.348
Energy to break (N·m)	47.894	57.169	57.95	73.099	71.962
Yield strength (N/mm ²)	33.469	40.819	53.559	44.726	38.66
Flexural strength (N/mm ²)	58.875	71.563	87.937	83.562	75.500
Elastic modulus of the composite (N/mm ²)	213.613	243.330	343.488	407.014	377.557
Hardness (HRB)	30.86	55.74	61.60	69.28	65.30

The composite exhibited fewer areas of stress concentration, resulting in a lower energy requirement to initiate cracks. Consequently, the impact strength was exceptionally high. However, when the biomass particulate content increased from 20% to 40%, the recycled LDPE began to fill the biomass particulate pores, restricting the movement of the recycled LDPE, which led to an increase in the rigidity and a decrease in the impact strength of the composite [27]. Consequently, as the biomass particulate content increased to 40%, less energy was necessary to withstand sudden impacts, resulting in a decline in impact energy. Another factor may have been the presence of numerous regions with poor stress concentration, making crack propagation easier in the composite samples [28]. Table 1 provides a comparison of the mechanical properties of the samples.

However, the increase in biomass (oyster shell and rice husk) contents posed challenges in achieving a uniform distribution of reinforcement. This finding is consistent with that of the review conducted by Yan *et al.* [29] who observed that the impact strength increased gradually until it reached its peak at 30% weight fraction of cloisite and cellulose fiber that have been recycled. Sarraj *et al.* [30] obtained similar results, with the maximum impact strength observed at 25% weight fraction of particulate fillers, after which it started to decline.

Compressive strength. Figure 3.18 illustrates the compressive strength of the composite materials. The 30% and 40% specimens exhibited values of 377.557 and 407.014 MPa, respectively. In contrast to tensile behavior, compressive behavior showed a distinct characteristic as the biomass particulates formed clusters, potentially enhancing microscopic mechanical interlocking.

In addition, the voids closed under compression, impeding crack propagation. Yoon and Kim observed a similar result in their study, in which oyster shell was used as reinforcement of cement composites [28]. The reinforced material exhibited the highest tensile strength and elastic modulus during compression, along with strain. According to other researchers, the incorporation of particulates, such as nanoclay, into the banana fibers resulted in a stronger bond at the interface between the banana fiber and the epoxy resin, which could be attributed to the decrease in the noncellulosic section of the fiber materials, ultimately enhancing the load-bearing capacity of the material. Similarly, Rahman *et al.* [31] reported that epoxy reinforced with a combination of particulates, such as nanoclay and graphene, along with carbon fibers of different volume fractions, exhibited similar behavior. The specimens that were reinforced with particulates, such as graphene, carbon fibers, and nanoclay, exhibited a compressive strength approximately 35% higher than that of the composite material that was reinforced with neat carbon fiber.

The compressive test conducted showed that the particulate-reinforced samples exhibited excellent performance. Generally, the particulates enhanced the strength at the particulate and matrix interface, thus improving the compressive properties [32].

Hardness analyses. To further elaborate on the findings, the hardness test provided additional insights. Although a slight variation was detected in the later stages, the 10%, 20%, and 30% specimens exhibited progressive results during the earlier stages of the test. However, a slight reduction of the hardness value with the addition of 40% biomass particulate occurred because of the agglomeration and uneven dispersion of particulate in the matrix. Nevertheless, both demonstrated comparable strength on compression, even at the region at which the composite material fails, which, therefore, indicates the superior load-bearing capabilities of the reinforced material.

4. Conclusion

Biomass particulates exhibit encouraging outcomes when used as reinforcements of a plastic matrix. Because of the hydrophobic properties of oyster shells, they can be evenly distributed throughout the plastic resin and adhere well to them. This characteristic is particularly noticeable in oyster shell/rice husk particulate BPC and shows in their thermal stability and viscoelastic behavior, especially at elevated temperatures.

The observations of the recorded TGA values and decomposition temperatures show that biomass-reinforced plastic composite exhibits thermal stability. The incorporation of biomass fiber/particulate into the PE plastic matrix not only increases the thermal stability but also reduces the energy dissipation. This finding can be attributed to the restricted movement of the polymer molecules at the interface. BPC containing 20wt% to 30wt% of biomass fiber particulates exhibits a higher storage modulus than unreinforced plastic composites as a result of the uniform dispersion of biomass particulates in the composite matrix.

The developed BPC material can be applied in the manufacturing process of electrical insulators and panels with improved thermal and electrical insulation and enhanced mechanical strength.

References

- [1] R.C. Thompson, C.J. Moore, F.S. Saal, S. H. Swan, *Philos. T. R. Soc. Lon. B.* 364/1526 (2009) 2153.
- [2] M. Eriksen, L.C.M. Lebreton, H.S. Carson, M. Thiel, C.J. Moore, J.C. Borerro, *et al.*, *PLoS One.* 9/12 (2014) e111913.
- [3] M. Pak, M.F. Türker, A. Öztürk, *Afr. J. Agric. Res.* 5/15 (2010) 1908.

- [4] C. Wilcox, E.V. Seville, B. Denise, *Proc. Nat. Acad. Sci.* 112/38 (2015) 11899.
- [5] S.O. Jekayinfa, J.I. Orisaleye, R. Pecenka, *Resources.* 9/8 (2020) 92.
- [6] S. Adiloğlu, *et al.*, *Intech. i/tourism* (2012) 13.
- [7] I.H. Rehman, *Enc. Energy.* 5 (2004) 507.
- [8] P. Hiremath, M. Shettar, M.C.G. Shankar, N.S. Mohan, *Mater Today-Proc.* 5/1 (2018) 3014.
- [9] C. Alia, J.A. Jofre-Reche, J.C. Suarez, J.M. Arenas, J.M. Martín-Martínez, *Polym. Degrad. Stabil.* 153 (2018) 88.
- [10] Z. Strakoš, *Found. Comput. Math.* 11 (2011) 241.
- [11] N. Khalid, M. Aqeel, A. Noman, S.M. Khan, N. Akhter, *Environ. Pollut.* 290 (2021) 118104.
- [12] A.L. Martínez-Hernández, C. Velasco-Santos, M. de-Icaza, V.M. Castaño, *Compos. Part B–Eng.* 38/3 (2007) 405.
- [13] J.A. Epaarachchi, In: R.M. Guedes (Ed.), *Creep and Fatigue in Polymer Matrix Composites*, Woodhead Publishing Series in Composites Science and Engineering, United Kingdom, 2011, p.492.
- [14] F. Carrasco, P. Pags, J. Gámez-Pérez, O.O. Santana, M.L. MasPOCH, *Polym. Degrad. Stabil.* 95/12 (2010) 2508.
- [15] A. Aboulkas, K. El harfi, A. El Bouadili, *Energ. Convers. Manage.* 51/7 (2010) 1363.
- [16] A. Acharya, E.H. Greener, *J. Dent. Res.* 51/5 (1972) 1363.
- [17] R. Kumar, S.M. Kumar, M.E.S. Kumar, V.R. Kumar, R. Kivade, J. Pavan, *et al.*, *Adv. Mater. Sci. Eng.* (2022) 1837741.
- [18] J. Brechtel, Y. Li, K. Li, L. Kearney, K. Nawaz, A. Flores-Betancourt, *et al.*, *Polymers*, 13/12 (2021) 1970.
- [19] PerkinElmer, *Dynamic Mechanical Analysis (DMA)–A Beginner’s Guide*, Introduction to DMA, PerkinElmer, Inc., USA, 2008.
- [20] A. Porbka, K. Jurkowski, J. Laska, *Polimery.* 60/4 (2015) 251.
- [21] K.B.N. Balasubramanian, T. Ramesh, *Polym. Advan. Technol.* 29/6 (2018) 1568.
- [22] H.T.N. Kuan, M.Y. Tan, Y. Shen, M.Y. Yahya, *Compos. Adv. Mater.* 30 (2021).
- [23] S. Zhang, Y. Yan, Y. Yang, R. Guo, *Molecules.* 29/3 (2024) 716.
- [24] S. Zhang, X. Wang, J. Yang, H. Chen, X. Jiang, *Int. J. Oral Sci.* 15/1 (2023) 21.
- [25] A.R. Prajapati, H.K. Dave, H.K. Raval, *Mater. Today-Proc.* 44/1(2021) 2102.
- [26] B.A. Salami, A.A. Bahraq, M.M. ul Haq, O.A. Ojelade, R. Taiwo, S. Wahab, *et al.*, *Next Materials.* 4 (2024) 100225.
- [27] L. Techawinyutham, J. Tengsuthiwat, R. Srisuk, W. Techawinyutham, S. Mavinkere Rangappa, S. Siengchin, *J. Mater. Res. Technol.* 15 (2021) 2445.
- [28] Y. Sun, T. Yan, C. Wu, X. Sun, J. Wang, X. Yuan, *Appl. Sci.* 8/11 (2018) 2093.
- [29] L. Yan, B. Kasal, L. Huang, *Compos. Part B–Eng.* 92 (2016) 94.
- [30] S. Sarraj, M. Szymiczek, T. Machoczek, M. Mrówka, *Polymers-Basel.* 13/7 (2021) 1103.
- [31] A.S. Rahman, V. Mathur, R. Asmatulu, *Compos. Struct.* 187 (2018) 481.
- [32] S.Y. Fu, X.Q. Feng, B. Lauke, Y.W. Mai, *Compos. Part B–Eng.* 39/6 (2008) 933.